

# Crack Influences on the Static and Dynamic Characteristic of a Micro-Beam Subjected to Electro Statically Loading

A.R. Shahani<sup>1,\*</sup>, G. Rezazadeh<sup>2</sup>, A. Rahmani<sup>1</sup>

<sup>1</sup>Department of Applied Mechanics, Faculty of Mechanical Engineering, K.N. Toosi University of Technology, Tehran, Iran

<sup>2</sup>Mechanical Engineering Departments, Urmia University, Urmia, Iran

Received 26 June 2018; accepted 23 August 2018

## ABSTRACT

In the present work the pull-in voltage of a micro cracked cantilever beam subjected to nonlinear electrostatic pressure was studied. Two mathematical models were employed for modeling the problem: a lumped mass model and a classical beam model. The effect of crack in the lumped mass model is the reduction of the effective stiffness of the beam and in the beam model; the crack is modeled as a massless rotational spring the compliance of which is related to the crack depth. Using these two models the pull-in voltage is extracted in the static and dynamic cases. Stability analysis is also accomplished. It has been observed that the pull-in voltage decreases as the crack depth increases and also when the crack approaches the clamped support of the beam. The finding of this research can further be used as a non-destructive test procedure for detecting cracks in micro-beams.

© 2018 IAU, Arak Branch. All rights reserved.

**Keywords:** MEMS; Cracked micro-beam; Stability analysis.

## 1 INTRODUCTION

**M**ICRO electromechanical systems (MEMS) are systems that consist of small-scale electrical and mechanical components designed for specific purposes. MEMS devices have attracted attentions in recent years because of their advantages such as light weight, small size, low-energy consumption and high accurate performance and also simple construction and their suitability with micro-fabrication technology. The micro-cantilever beams are widely used in micro-electromechanical systems. The micro-cantilever beams are the main part of Micro-actuators such as Capacitive Micro-switches. The electrostatic actuators are deformable condensers and often made of two parts: one deformable electrode and one or more fixed electrodes. Application of voltage between the fixed electrodes and deformable electrode induces electrostatic forces that result in deformation of deformable electrodes [1]. The electrostatic actuation is used greatly as a provoking in electrostatic actuators such as capacitive micro-switches, resonate sensor and optical scanner [2]. Elata and Bamberger [3] studied the dynamic response of electrostatic actuators with multiple DOF that are driven by multiple voltage sources. Zhang and Zhao [4] used the one-mode analysis method to find out the pull-in voltage and displacement. They showed that for low axial loading range, this method shows a little difference in the established multi-mode analysis on predicting the pull-in voltage. Rezazadeh et al. [5] studied the static behavior of a fixed-fixed and cantilever micro-beam using both of the lumped and distributed models to the DC voltage. By the use of step by step linearization method (SSLM) they solved the

\*Corresponding author. Tel.: +98 21 840 63221; Fax.: +98 21 886 77 273.  
E-mail address: [shahani@kntu.ac.ir](mailto:shahani@kntu.ac.ir) (A.R. Shahani).

governing static equation and then they offered the closed-form solution for calculation of pull-in voltage. Pull-in instability as an inherently nonlinear and crucial effect continues to become increasingly important for the design of electrostatic MEMS and NEMS devices and ever more interesting scientifically [6]. Choi and Lovell [7] calculated numerically the static deflection of micro-beam using a shooting method. Their model consists of electrostatic force and mid-plane stretching force. Chowdhury et al. [8] proposed the closed-form solution for pull-in voltage in micro cantilever beams too.

When the rate of voltage variation is not negligible, the effect of inertia has to be considered. The pull-in instability related to this situation is called dynamic pull-in instability and the critical value of voltage, corresponding to the dynamic instability, is called dynamic pull-in voltage. Chao et al. [9] have investigated DC dynamic pull-in instability for a generalized clamped-clamped micro beam based on a continuous model and bifurcation analysis. Krylov [10] has investigated the dynamic pull-in instability of micro beam subjected to nonlinear squeeze film damping using a reduced order model. Silicon and Silicon-based micro-beams are the most frequently used in MEMS devices such as pressure sensors, accelerometers, RF micro switches and so forth. These micro-beams are often subjected to destructive mechanical and chemical environments. In spite of a decade of investigation on fatigue failure of silicon-based materials, failure mechanism of micro-scale thin silicon micro-beams is not fully studied [11]. Silicon is a brittle material at room temperature. In the absence of hydrostatic confining pressures to suppress fracture, silicon display no dislocation activity, even at high stresses [12] thus silicon display no time-dependent cracking when subjected to cyclic loading conditions. However, experimental results have shown otherwise. Silicon-based micro-beams degrade and fail under cyclic loading condition in ambient air and at room temperature [13, 14]. Crack initiation and growth have also been reported in micro-sized silicon films even in the absence of pre-cracks under fatigue loading [13]. Fatigue failure mechanism of silicon-based microfilms has been described by two distinct methodologies in the literature [11]. In first methodology, the microfilms of silicon subjected to cyclic tension/compression loading undergo fatigue and could ultimately fail as a result of damage produced by compressive reversals, rather than environment stress corrosion cracking. The second mechanism suggests that the fatigue of silicon-based microfilms occurs through a process of sequential, mechanically induced oxidation and environmentally assisted cracking of the surface layer of material that forms upon reaction with atmosphere that is termed as reaction-layer fatigue. This progressive accumulation of fatigue damage is accompanied with a decrease in the stiffness of microfilms of silicon materials.

Motallebi et al. [15] studied the effects of the open crack on the static and dynamic pull-in voltages of electrostatically actuated micro-beams. They solved the governing static and dynamic equations by Galerkin-based Reduced Order Model. Each single-side open crack in the micro-beam is modeled by a massless rotational spring and the cracked mode shapes and corresponding natural frequencies are calculated by considering the boundary and patching conditions and using transfer matrix methods. Their results show that the existence defects such as crack, leads to reduction of the stiffness of micro-beam and consequently decreases the natural frequencies. Sourki and Hoseini [16] investigated the analysis for free transverse vibration of a cracked micro-beam based on the modified couple stress theory within the framework of Euler–Bernoulli beam theory. The cracked beam is modeled by dividing the beam into two segments connected by a rotational spring located at the cracked section. In this investigation, the influence of diverse crack position, crack severity, material length scale parameter as well as various Poisson's ratio on natural frequencies is studied. Transverse vibration of cracked nano-beam has been studied based on modified couple stress theory by Tadi Beni et al. [17]. They modeled the crack discontinuity by a rotational spring and found that the effects of the crack parameter and crack location on transverse frequency of the cracked nano-beam are quite significant. Nonlocal cracked-rod model is used to analysis the torsional vibrations of a carbon nano-tube with a circumferential crack by Loya et al. [18]. In their work, the cracked rod is modeled by dividing the cracked element into two segments connected by a torsional linear spring whose stiffness is related to the crack severity. Barr and Christides [19] derived the differential equation and associated boundary conditions for a uniform Euler-Bernoulli beam containing a pair of symmetric cracks using Hu-washizu principle. They introduced the effect of crack in the form of perturbation in the stresses, strains, displacements and momentum fields as a local function which assumes an exponential decrease with the axial distance from the crack. Measuring the flexural vibrations of a cracked cantilever beam and comparing their results with the analytical results of Rizos et al. [20], they were able to detect the location and depth of the crack in the beam. Chondros et al. [21] developed continuous cracked beam vibration theory for the vibration of Euler-Bernoulli beams. The Hu-Washizu-Barr variational formulation was used to develop the differential equation and boundary conditions of the cracked beam. Behzad et al. [22] presented a new linear theory for bending stress-strain analysis of a cracked beam. Li [23] proposed an exact approach for free vibration analysis of a non-uniform beam with an arbitrary number of cracks and concentrated masses. Binici [24] proposed a new method to obtain the Eigen frequencies and mode shapes of beams containing

arbitrary number of cracks and subjected to axial force. The author supposed that the cracks introduce local flexibility and are modeled as rotational springs.

The general issue is the susceptibility of the silicon-based micro-beams to expose the micro-cracks. The formation of micro-cracks would gradually change the resonant frequency and electrical resistance of micro-devices, degrade the sensor output and, most seriously, lead to the failure of MEMS devices [25]. So, modeling the effect of cracks on mechanical behavior of micro-beams is worthy of investigation. It worth pointing out that, in microstructures, the size effect cannot be interpreted implicitly by beam models based on classical (macro) elasticity theories due to lack of material length scale parameters. Then, higher order continuum (nonlocal) theories, which contain additional material length scale parameters besides the classical material constants (Lame) have been proposed to predict the size dependence of these nano/micro-structures. Mostly generally known higher order theories are the micro-polar (Cosserat) elasticity, nonlocal theory of Eringen, strain gradient elasticity and couple stress theories [26]. The silicon is the most common material in the MEMS/NEMS devices. Sadeghian et al. [27] experimentally showed that the size-dependent mechanical properties for a silicon beam are significant as the beam thickness approaches nano-meter scale. Therefore, as the scales of the structure in this study are considered in the range of micro, the material length scale can be neglected, in other words,  $\ell \cong 0$  ( $\ell$  refers to length scale parameter) [28]. Therefore, the effective elasticity modulus can be considered equal to the classic modulus of silicon. Free vibration of edge cracked functionally graded micro scale beams based on the Modified couple stress theory investigated by Akbas [29]. The cracked beam is modeled as a modification of the classical cracked-beam theory consisting of two sub-beams connected by a massless elastic rotational spring. They concluded that the crack location and crack depth play an important role in the vibration response of the FG micro beams. Torabi and Dastgerdi [30] published an analytical method for free vibration analysis of Timoshenko beam theory applied to cracked nano-beams using a nonlocal elasticity model. They obtained frequencies and vibration mode of cracked nano-beams.

In spite of many efforts for investigating the behavior of cracked beams, there are a few studies on the behavior of micro-cracked beam devices in literature. Then, this paper is devoted to the investigation of the behavior of micro cracked beams under electro-statically actuation. A massless rotational spring model has been used to describe the local flexibility induced by the crack in the beam. The mode shape function of per segment of the beam has been derived using the fundamental solutions and recurrence formulas. The main advantage of this method is that it is applicable for a non-uniform beam with any number of cracks and any kind of boundary conditions. Static and dynamic analyses have been performed for extracting the deflection of the beam and also, the pull-in voltage, the voltage in which the system becomes unstable. On the other hand, a lumped mass model has been derived for the system for the purpose of verification of the results. Stability analysis has been accomplished using both the 1DOF and the beam model. The results have been compared, in the special case of a beam without any crack, with those cited in the literature showing good agreement. It has been concluded that the pull-in voltage decreases with the crack depth increase. On the other hand, when the crack approaches the clamped end of the beam, the pull-in voltage experiences further decrease. The results of the present investigation can also be used as set points for a non-destructive testing procedure for detecting crack in a micro-cantilever beam.

## 2 MODEL DESCRIPTION AND ASSUMPTIONS

In order to analyze the effects of an edge crack on the mechanical behavior of a MEMS switch, a cantilever micro-beam subjected to a nonlinear electrostatic pressure is considered (Fig. 1).

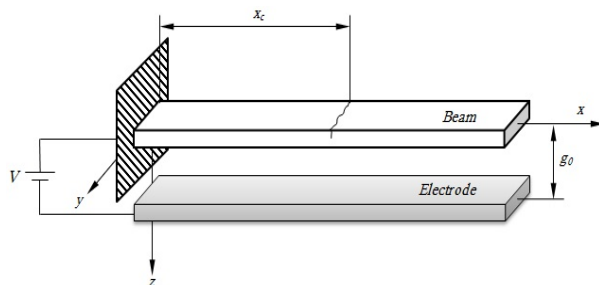


**Fig.1**  
An electrostatically-actuated micro cantilever beam with an edge crack.

The micro-beam is considered to be isotropic and homogenous with a length  $L$ , width  $b$  and thickness  $h$ . The micro-beam has a crack with a depth  $a$  at the position  $x = x_c$ .

The micro-beam is considered to be suspended over a stationary electrode (substrate) and is subjected to an actuation voltage  $V$ . Initial gap between the micro-beam and the stationary electrode is  $g_0$ . When a voltage is applied to the micro-beam and substrate, the attractive electrostatic force pulls the micro-beam toward the stationary electrode. When the voltage is increased, the distance of the two beams is decreased. As the voltage is reached to a critical value which is known as the pull-in voltage, the movable beam abruptly collapses to the substrate.

The electrostatic actuation exerted on the capacitor introduces an electric energy  $W_e$  and complementary energy  $W_e^*$  [1]:

$$W_e = \int_0^q V dq = \int_0^q \frac{q}{C} dq = \frac{q^2}{2C}, \quad W_e^* = \int_0^q q dV = \frac{\varepsilon_0 A V^2}{2(g_0 - w)} \quad (1)$$

In which the following relations are used

$$q = CV, \quad C = \frac{\varepsilon_0 A}{d} \quad (2)$$

The electrostatic attraction force  $F_e$  between the movable plate and fixed ground plate can be obtained by differentiating the energy stored in the capacitor structure with respect to the deflection of the movable plate as:

$$F_e = \frac{\partial W_e^*}{\partial w} = \frac{\varepsilon_0 A V^2}{2(g_0 - w)^2} \quad (3)$$

In Eq. (3),  $A = b \cdot L$  is the capacitor surface and  $\varepsilon_0$  is the permittivity of the dielectric medium and  $F_e$  is the total value of the electrostatic force. Severity of this force per unit length of the micro-beam is written as:

$$f_e = \frac{F_e}{L} = \frac{\varepsilon_0 b V^2}{2(g_0 - w)^2} \quad (4)$$

The governing equation for the dynamic behavior of the micro-cantilever beam, subjected to non-uniform electrostatic force, can be expressed as:

$$\tilde{E}I \frac{\partial^4 w}{\partial x^4} + \rho A \frac{\partial^2 w}{\partial t^2} = f_e(w, V) = \frac{\varepsilon_0 b V^2}{2(g_0 - w)^2}; \quad 0 < x < L \quad (5)$$

The beam is considered wide when  $b \geq 5h$ . Wide beams exhibit plane-strain conditions and therefore, effective modulus  $\tilde{E}$  becomes  $E/(1-\nu^2)$ , where  $E$  and  $\nu$  are the Young's modulus and Poisson's ratio, respectively. A beam is considered narrow, when  $b \geq 5h$ . For this case effective modulus  $\tilde{E}$  becomes  $E$ .  $I$  is the moment inertia of the cross-section,  $\rho$  is the density,  $\varepsilon_0$  and  $g_0$  is the dielectric constant of the gap medium and the initial gap, respectively.

### 3 SOLUTION OF THE PROBLEM

Eq. (5) is a nonlinear differential equation which must be solved with an iterative numerical procedure. For this to be achieved, we applied two steps for our solution. At first by applying step by step linearization method (SSLM), the nonlinear governing equation is reduced to an ordinary differential equation in each step of solution then for solving these ordinary differential equations Galerkin procedure was employed. Using free flexural vibration shape

functions for micro cracked cantilever beam, which satisfy the boundary conditions, the static and dynamic solution is investigated.

### 3.1 Derivation of the shape functions for a cracked beam

In this part, at first the shape functions of a cracked beam are extracted and using these shape functions the displacement of the micro beam and static and dynamic pull-in voltage of the system are calculated.

The following assumptions are considered for the cracked beam:

- The beam is slender.
- The crack is considered to be stationary open edge narrow notch with parallel faces.
- The deformations are supposed to be small.
- The plane strain assumption has been used.
- The material is assumed to be linear elastic.
- It is assumed that the crack faces do not contact in the loading process.

For Euler-Bernoulli beam the differential equation of free flexural vibration of an un-cracked beam is:

$$\tilde{E}I \frac{\partial^4 w}{\partial x^4} + \rho A \frac{\partial^2 w}{\partial t^2} = 0 \quad (6)$$

Eq. (6) can be solved using the separation of variables technique of the form:

$$w(x, t) = Y(x) e^{i\omega t} \quad (7)$$

Substituting Eq. (7) in Eq. (6) yields:

$$EI \frac{\partial^4 Y}{\partial x^4} - \rho A \omega^2 Y = 0; \quad (8)$$

In Eq. (8),  $\omega$  is the circular natural frequency of the transverse vibration. The general solution for Eq. (8) can be written in terms of some constants representing the boundary conditions of the beam at  $x=0$ :

$$Y(\chi) = Y(0)A(\chi) + Y'(0)B(\chi) + Y''(0)C(\chi) + Y'''(0)D(\chi); \quad (9)$$

In Eq. (9),  $\chi$  is the non-dimensional length parameter ( $x/L$ ), and the parameters  $Y(0)$ ,  $Y'(0)$ ,  $Y''(0)$ ,  $Y'''(0)$  correspond to the boundary conditions. These relations are given as:

$$Y'(0) = \theta(0)L; \quad Y''(0) = \frac{M(0)L^2}{EI}; \quad Y'''(0) = \frac{Q(0)L^3}{EI}; \quad (10)$$

where  $\theta(0)$ ,  $M(0)$ ,  $Q(0)$  are slope, moment and shear force at  $\chi=0$ , respectively. The functions  $A(\chi)$ ,  $B(\chi)$ ,  $C(\chi)$ ,  $D(\chi)$  are non-dimensional functions which are selected linearly independent. They must satisfy the following conditions:

$$\begin{bmatrix} A(0) & A'(0) & A''(0) & A'''(0) \\ B(0) & B'(0) & B''(0) & B'''(0) \\ C(0) & C'(0) & C''(0) & C'''(0) \\ D(0) & D'(0) & D''(0) & D'''(0) \end{bmatrix} = \begin{bmatrix} 1 & 0 & 0 & 0 \\ 0 & 1 & 0 & 0 \\ 0 & 0 & 1 & 0 \\ 0 & 0 & 0 & 1 \end{bmatrix} \quad (11)$$

Eq. (8) can be solved to yield the following forms for the above mentioned functions [24]:

$$\begin{aligned} A(\chi) &= \frac{1}{2}[\cosh(\alpha\chi) + \cos(\alpha\chi)] \\ B(\chi) &= \frac{1}{2\alpha}[\sinh(\alpha\chi) + \sin(\alpha\chi)] \\ C(\chi) &= \frac{1}{2\alpha^2}[\cosh(\alpha\chi) - \cos(\alpha\chi)] \\ D(\chi) &= \frac{1}{2\alpha^3}[\sinh(\alpha\chi) - \sin(\alpha\chi)] \end{aligned} \quad (12)$$

In which  $\alpha = \sqrt[4]{\left(\frac{\rho A}{EI}\right)(\omega L^2)^2}$ . Due to the presence of the crack, the deflection of the beam should be presented with two different functions  $Y_1(\chi)$ ,  $Y_2(\chi)$ . The expression for the first part of the beam (before the crack) is as follows:

$$Y_1(\chi) = Y_1(0)A(\chi) + Y_1'(0)B(\chi) + Y_1''(0)C(\chi) + Y_1'''(0)D(\chi) \quad (13)$$

The boundary conditions at  $\chi = 0$  can be used to reduce Eq. (13) to a form which includes only two of initial parameters. A model of massless rotational spring is adopted for the crack to describe the local flexibility due to the presence of the crack [24, 31- 32]. According to this method, it is required that continuity of displacement, moment, and shear force to be satisfied. Also jump condition for the slope at the position of the crack needs to be satisfied due to the presence of the rotational spring. The continuity conditions of the beam at the crack position can be expressed as:

$$\begin{aligned} Y_1(\chi_c) &= Y_2(\chi_c) \\ Y_1''(\chi_c) &= Y_2''(\chi_c) \\ Y_1'''(\chi_c) &= Y_2'''(\chi_c) \end{aligned} \quad (14)$$

Jumping condition of the slope is as:

$$Y_2'(\chi_c) - Y_1'(\chi_c) = C_1 Y_1''(\chi_c) \quad (15)$$

In Eq. (15),  $C_1$  is the non-dimensional flexibility of the rotational spring representing the effect of the crack at the location  $\chi_c$ . For a one sided open crack,  $C_1$  is given in the following form [28-29]:

$$\begin{aligned} C_1(a/h) &= 5.346(h/L)[1.8624(a/h)^2 - 3.95(a/h)^3 + 16.375(a/h)^4 - 37.226(a/h)^5 \\ &+ 76.81(a/h)^6 - 126.9(a/h)^7 + 172(a/h)^8 - 143.97(a/h)^9 - 66.56(a/h)^{10}] \end{aligned} \quad (16)$$

In Eq. (16),  $a$  is the depth of the crack and  $h$  is the depth of the beam section and  $L$  refers to the length of the beam. In order to satisfy the jump condition of the slopes (Eq. (15)), and the continuity of shear at the crack location, the following expression needs to hold [24]:

$$Y_2(\chi) = Y_1(\chi) + C_1 Y_1''(\chi_c) B(\chi - \chi_c) \quad (17)$$

It can be seen that when  $\chi = \chi_c$  then  $B(0) = 0$ ,  $B'(0) = 1$ ,  $B''(0) = 0$ ,  $B'''(0) = 0$ . It means that all the conditions at the crack location are satisfied. This method is very general and it could be used for any number of cracks. If we focus our study on the cantilever beam with a single edge crack (Fig. 1), application of the boundary conditions at the starting point of the beam yield the mode shape functions for each segment in the following form:

$$\begin{aligned} Y_1(\chi) &= Y_1''(0)C(\chi) + Y_1'''(0)D(\chi) \\ Y_2(\chi) &= Y_1(\chi) + C_1 Y_1''(\chi_1)B(\chi - \chi_1) \end{aligned} \quad (18)$$

The boundary conditions corresponding to the free end of the beam are as follows:

$$Y_2''(1) = 0, \quad Y_2'''(1) = 0 \quad (19)$$

Applying Eqs. (19) on (18), leads to:

$$\begin{bmatrix} S_1 & S_2 \\ S_3 & S_4 \end{bmatrix} \begin{bmatrix} Y_1''(0) \\ Y_1'''(0) \end{bmatrix} = \begin{bmatrix} 0 \\ 0 \end{bmatrix} \quad (20)$$

where

$$\begin{aligned} S_1 &= \left(\frac{1}{2}[\cosh(\alpha) + \cos(\alpha)]\right) + C_1 \left(\frac{1}{2}[\cosh(\alpha\chi_c) + \cos(\alpha\chi_c)]\right) * \left(\frac{\alpha}{2}[\sinh(\alpha(1-\chi_c)) - \sin(\alpha(1-\chi_c))]\right) \\ S_2 &= \left(\frac{1}{2\alpha}[\sinh(\alpha) + \sin(\alpha)]\right) + C_1 \left(\frac{1}{2\alpha}[\sinh(\alpha\chi_c) + \sin(\alpha\chi_c)]\right) * \left(\frac{\alpha}{2}[\sinh(\alpha(1-\chi_c)) - \sin(\alpha(1-\chi_c))]\right) \\ S_3 &= \left(\frac{\alpha}{2}[\sinh(\alpha) - \sin(\alpha)]\right) + C_1 \left(\frac{1}{2}[\cosh(\alpha\chi_c) + \cos(\alpha\chi_c)]\right) * \left(\frac{\alpha^2}{2}[\cosh(\alpha(1-\chi_c)) - \cos(\alpha(1-\chi_c))]\right) \\ S_4 &= \left(\frac{1}{2}[\cosh(\alpha) + \cos(\alpha)]\right) + C_1 \left(\frac{1}{2\alpha}[\sinh(\alpha\chi_1) + \sin(\alpha\chi_c)]\right) * \left(\frac{\alpha^2}{2}[\cosh(\alpha(1-\chi_c)) - \cos(\alpha(1-\chi_c))]\right) \end{aligned} \quad (21)$$

Non-trivial solution of the set of Eqs. (20) can be obtained by putting the determinant of the coefficient matrix equal to zero. The resulting equation gives the Eigen frequencies of the cracked beam and also the shape functions for each segment of the beam.

### 3.2 Static analysis

In this section we proposed solution method with introducing the crack effect in the static solution. This method consists of two stages: at first, the step by step linearization method (SSLM) is applied to the nonlinear differential equation and then the Galerkin based weighted residual method is used to discretize the resultant linear differential equation. For using this method, the variations of parameters are considered in the following form [35]:

$$w_{i+1} = w_i + \delta w = w_i + \psi(x), \quad V_{i+1} = V_i + \delta V \quad (22)$$

In Eq. (22),  $\psi(x)$  is an unknown function which should be determined in each step:

Step  $i$ :

$$EI \frac{d^4 w_i}{dx^4} = \frac{\varepsilon_0 b V_i^2}{2(g_0 - w_i)^2} \quad (23)$$

Step  $i + 1$ :

$$EI \frac{d^4 w_{i+1}}{dx^4} = \frac{\varepsilon_0 b V_{i+1}^2}{2(g_0 - w_{i+1})^2} \quad (24)$$

Considering Taylor series expansion of the electrostatic force in Eq. (24) about the static equilibrium position in step  $i$ , i.e.,  $w_i$  results in:

$$\frac{\varepsilon_0 b V_{i+1}^2}{2(g_0 - w_{i+1})^2} = \frac{\varepsilon_0 b V_{i+1}^2}{2(g_0 - w_i)^2} + \frac{\varepsilon_0 b V_{i+1}^2}{2(g_0 - w_i)^3} \psi(x) + O(2) \quad (25)$$

It can be noted that in this expansion, only two terms of the series is considered. Substituting Eqs. (22), (23) and (24) in Eq. (25) yields:

$$EI \frac{d^4 w_{i+1}}{dx^4} = EI \frac{d^4 w_i}{dx^4} + EI \frac{d^4 \psi(x)}{dx^4} = \frac{\varepsilon_0 b V_{i+1}^2}{2(g_0 - w_{i+1})^2} = \frac{\varepsilon_0 b V_{i+1}^2}{2(g_0 - w_i)^2} + \frac{\varepsilon_0 b V_{i+1}^2}{(g_0 - w_i)^3} \psi(x) \quad (26)$$

Subtracting Eq. (23) from Eq. (26) leads to the following linear differential equation:

$$EI \frac{d^4 \psi(x)}{dx^4} - \frac{\varepsilon_0 b V_{i+1}^2}{(g_0 - w_i)^3} \psi(x) = \frac{\varepsilon_0 b (V_{i+1}^2 - V_i^2)}{2(g_0 - w_i)^2} \quad (27)$$

Now, for solving this equation, Galerkin weighted residual method is utilized. In this method, the solution is approximated as:

$$\psi(x) = \sum_{n=1}^N a_n \varphi_n(x) \quad (28)$$

In this equation  $\varphi_n(x)$  are the shape functions for the cracked beam, as derived in Eq. (18).  $a_n$ 's are unknown coefficients which should be determined. Substituting the approximated solution into Eq. (27), leads to the following residual:

$$R_1 = \sum_{n=1}^N EI a_n \varphi_n^{(4)} - \frac{\varepsilon_0 b V_{i+1}^2}{(g_0 - w_i)^3} \sum_{n=1}^N a_n \varphi_n - \frac{\varepsilon_0 b (V_{i+1}^2 - V_i^2)}{2(g_0 - w_i)^2} \quad (29)$$

Based on the Galerkin weighted residual method,  $a_n$  can be determined in such a manner the weighted integral of the problem vanishes:

$$\int_0^l \varphi_m R_1 dx = 0, \quad m=1,2,\dots,N \quad (30)$$

Applying Eq. (29) on Eq. (30) leads to:

$$\sum_{n=1}^N K_{mn} a_n = F_m, \quad m=1,2,\dots,N \quad (31)$$

where

$$K_{mn} = \int_0^l \varphi_m \left[ \sum_{n=1}^N EI \varphi_n^{(4)} - \frac{\varepsilon_0 b V_{i+1}^2}{(g_0 - w_i)^3} \sum_{n=1}^N \varphi_n \right] dx, \quad F_m = \int_0^l \varphi_m \left[ \frac{\varepsilon_0 b (V_{i+1}^2 - V_i^2)}{2(g_0 - w_i)^2} \right] dx \quad (32)$$

Eq. (31) is a set of  $N$  equations which can be solved to give  $N$  unknowns  $a_n$ . After finding  $a_n$ 's, one can compute  $\psi(x)$  and as a result  $w(x)$  in each step of DC voltage application.

### 3.3 Dynamic analysis

In this section the instability of dynamic pull-in is studied, when a step DC voltage is applied on the cracked beam. The geometric parameters of the problem are  $L = 100 \mu\text{m}$ ,  $x_c = 0$ , and  $a = 1.5 \mu\text{m}$ . The dynamic equation of the deflection of the beam subjected to electrostatic step DC voltage is as follows:

$$EI \frac{\partial^4 w}{\partial x^4} + \rho A \frac{\partial^2 w}{\partial t^2} = \frac{\varepsilon_0 b V_{dc}^2}{2(g_0 - w)^2} \quad (33)$$

For convenience, the following non-dimensional parameters are introduced (denoted by hats):

$$\hat{w} = \frac{w}{g_0}, \quad \hat{x} = \frac{x}{L}, \quad \hat{t} = \frac{t}{T}, \quad T = \sqrt{\frac{\rho b h L^4}{EI}}$$

Applying the non-dimensional parameters on Eq. (33) leads to:

$$\frac{\partial^4 \hat{w}}{\partial \hat{x}^4} + \frac{\partial^2 \hat{w}}{\partial \hat{t}^2} = \alpha \frac{V_{dc}^2}{2(1 - \hat{w})^2} \quad (34)$$

where:

$$\alpha = \frac{6\varepsilon_0 L^4}{Eh^3 g_0^3}$$

Next, we generate a reduced-order model by discretizing Eq. (34) to a finite-degree-of-freedom system consisting of ordinary-differential equations in time. The un-damped linear mode shapes of the straight micro cracked beam can be used as the base functions in the Galerkin procedure. To this end, we express the deflections as:

$$\hat{w}(x, t) = \sum_{n=0}^N U_n(t) \varphi_n(x) \quad (35)$$

where  $U_n(t)$  is the  $n^{\text{th}}$  generalized coordinate and  $\varphi_n(x)$  is the  $n^{\text{th}}$  linear un-damped mode shape of the straight micro cracked beam. Substituting Eq. (35) in Eq. (34) yields:

$$\sum_{n=0}^N U_n(t) \varphi_n^{(4)}(x) + \sum_{n=0}^N \ddot{U}_n(t) \varphi_n(x) = \alpha \frac{V_{dc}^2}{2(1 - \hat{w})^2} \quad (36)$$

Multiplying Eq. (36), by  $\varphi_m(x)$  and integrating the outcome from  $x = 0$  to 1 yield the reduced-order model.

$$\int_0^1 \sum_{n=0}^N \varphi_m (U_n \varphi_n^{(4)} + \ddot{U}_n \varphi_n) dx = \int_0^1 \alpha \frac{V_{dc}^2}{2(1 - \hat{w})^2} \varphi_m dx \quad (37)$$

or in a more convenient form:

$$M_{mn} \ddot{U}_n(t) + K_{mn} U_n(t) = F_m \quad (38)$$

where

$$M_{mn} = \int_0^1 \varphi_m \varphi_n dx, \quad K_{mn} = \int_0^1 \varphi_m \varphi_n^{(4)} dx, \quad F_m = \int_0^1 \alpha \frac{V_{dc}^2}{2(1 - \hat{w})^2} \varphi_m dx$$

Now, Eq. (38) can be integrated over time by various integration methods such as Runge-Kutta method.

#### 4 LUMPED MODEL ANALYSIS

Because of complexity of the model of the air-gap capacitor, which makes it unsuitable for quick design calculations, it would be attractive to have a simple model to predict the static and dynamic behavior of the micro beam with sufficient accuracy. A lumped spring-mass system is proposed for studying the micro-beams [36]. Herein, the lumped mass model is employed for verifying the continuous model results and instability analysis of the system.

An appropriate way for the determination of equivalent spring constant ( $k_{eff}$ ) could be defined as the spring constant of a beam subjected to uniform load  $q_0$ . The pull-in voltage can be easily derived based on the balance of spring force and electrostatic force. According to Fig. 2 at the static equilibrium position the electrostatic force is balanced with spring force, i.e.:

$$k_{eff} x = \frac{\epsilon_0 A V^2}{2(g_0 - x)^2} \quad (39)$$

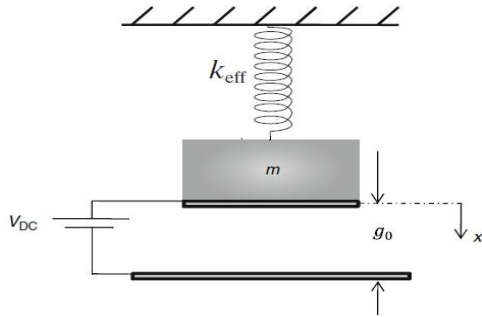


**Fig.2**  
Lumped model for micro cracked cantilever beam.

where  $x$  parameter in this equation is related to the displacement of the 1DOF system at the applied voltage. This cubic equation can be solved respect to  $x$ . This equation is solved by [1, 37-38] to give the critical values that are called pull-in voltage and pull-in position in following form:

$$V_{PI} = \sqrt{\frac{8k_{eff} g_0^3}{27\epsilon_0 A}} \quad , \quad x_{PI} = \frac{2}{3} g_0 \quad (40)$$

with the above procedure equivalent stiffness  $k_{eff}$  for intact cantilever beam is given by the following relation [38-40]:

$$k_{eff} = \frac{2Eb}{3} \left( \frac{h}{L} \right)^3 \quad (41)$$

But for the micro cracked cantilever beam the finite element method is employed to determine the stiffness of the beam. The crack is supposed to be located at the support and the properties of the micro beam are given in Table 1.

**Table 1**  
Material properties and Geometry of the micro-beam (single-crystal silicon).

Young's modulus ( $E$ )	169GPa
Density ( $\rho$ )	2331Kg/m <sup>3</sup>
Poisson's ratio ( $\nu$ )	0.06
Length ( $L$ )	100 $\mu$ m
Width ( $b$ )	50 $\mu$ m
Thickness ( $h$ )	3 $\mu$ m
Initial gap ( $g_0$ )	1 $\mu$ m
Permittivity of air	8.85 PF/m

The resultant equivalent stiffness for different crack depths at  $x = 0$  position is listed in Table 2.

**Table 2**

Equivalent stiffness for lumped model of a cracked cantilever beam with  $L = 100\mu\text{m}$ ,  $x_c = 0$ .

Crack depth	$a = 0\mu\text{m}$	$a = 0.5\mu\text{m}$	$a = 1\mu\text{m}$	$a = 1.5\mu\text{m}$
$k_{eff}$	148.02	144.1707	132.926	120.036

#### 4.1 Stability analysis and phase portrait for 1DOF model

A powerful method to understand the behavior and stability of a dynamical system is through the so-called phase portrait method. The equation of motion of the micro beam in the lumped model actuated by a step DC voltage can be written as follows:

$$m_{eff}\ddot{x} + k_{eff}x = \frac{\varepsilon AV^2}{2(g_0 - x)^2} \quad (42)$$

where  $A = b \cdot L$  is electrode area on the microstructure. For convenience, the non-dimensional parameters are introduced:

$$\hat{x} = \frac{x}{g_0}, \quad \hat{t} = \frac{t}{T}, \quad T^2 = \frac{m_{eff}}{k_{eff}}$$

where  $T$  is the time period of 1DOF model. Applying these changes of variables to Eq. (42) yields:

$$\ddot{\hat{x}} + \hat{x} = \frac{\alpha V^2}{(1 - \hat{x})^2} \quad (43)$$

where

$$\alpha = \frac{\varepsilon_0 A}{2g_0^3 k_{eff}}$$

In order to analyze the stability of the model, at first we calculate the fixed points of the system. For convenience we drop hats in Eq. (43). Letting  $x_1 = \dot{x}$  and  $x_2 = x$ , Eq. (43) is written in state-space as follows:

$$\dot{x}_1 = x_2 \quad \dot{x}_2 = \frac{\alpha V^2}{(1 - x_1)^2} - x_1 \quad (44)$$

The equilibrium points are obtained setting the Eq. (44) equal to zero. Therefore:

$$x_2 = 0 \quad x_1^3 - 2x_1^2 + x_1 - \alpha V^2 = 0 \quad (45)$$

Solving Eq. (45) gives three solutions for  $x_1(x_{11}, x_{12}, x_{13})$ . From these solutions  $x_{11}, x_{12}$  is in interval  $[0, 1]$  but  $x_{13}$  is negative and so, it is physically impossible solution. In this step, to analysis the stability, the Jacobian of Eq. (44) is calculated:

$$\nabla_x F = \begin{bmatrix} 0 & 1 \\ \frac{2\alpha V^2}{(1 - x_1)^3} - 1 & 0 \end{bmatrix} \quad (46)$$

The characteristic equation can be obtained as follows:

$$|\nabla_x F - \lambda I| = 0 \tag{47}$$

where  $I$  is the diagonal identity matrix. Eq. (47) yields a characteristic algebraic equation for  $\lambda$ , which is solved to yield the eigenvalues of the system as:

$$\lambda_{1,2} = \pm \sqrt{\frac{2cV^2}{(1-x_1)^3} - 1} \tag{48}$$

The variation of eigenvalues versus applied voltage is shown in the next chapter and then the stability of the system is analyzed.

### 5 RESULTS AND DISCUSSIONS

To show the numerical results of the analysis presented in previous sections, a micro-beam with specifications introduced in Table 1. is considered.

#### 5.1 Static pull-in voltage using 1DOF model

The displacement versus applied voltage is shown in Fig. 3. As Fig. 3 shows, for a given applied voltage there exists three equilibrium positions (fixed points), the first is a stable centre, the second is unstable saddle node and the third is a mathematically stable center but physically impossible. The impossibility of the third stable solution refers to the existence of the substrate, which restricts the amplitude of the micro beam motion.

In simple terms, the pull-in voltage  $V_{pi}$  can be defined as the voltage at which the restoring spring force can no longer balance the attractive electrostatic force. As can be seen (Fig. 3) in micro cracked beam with increasing the crack depth, pull-in voltage decreases. It is obvious that with increasing crack depth, the stiffness of the beam at the tip point of the micro beam is decreased. This decreasing of stiffness leads to instability voltage (pull-in voltage) decrease (Fig. 3).

On the other hand, as is seen from the Fig. 3, when no crack exists the results coincide with those of Younis [38].

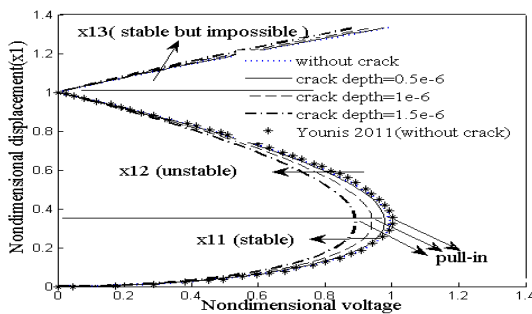


**Fig.3** Variation of non-dimensional displacement versus non-dimensional voltage.

#### 5.2 Static pull-in voltage using beam model

In this section, solution of Eq. (24) for different states of depth and location of the crack is illustrated. The resultant pull-in voltages for a crack lying at  $x_c = 0.5$  with different lengths are given in Table 3.

**Table 3** Pull-in voltage versus depth of the crack locating at  $x_c = 0.5$ .

Crack depth	$0\mu m$	$0.5\mu m$	$1\mu m$	$1.5\mu m$
$V_{pi}(V)$	38.20	38.2	38	37.8

It is seen that the result for the beam without any crack ( $a = 0$ ) is the same as that reported by Osterberg [41]. Another example has been considered for the case of  $x_c = 0$ . Table 4. shows the pull-in voltages for different crack depths. Again it is seen that the pull-in voltage for a beam without any crack is exactly the same as that reported by Osterberg [41].

**Table 4**  
Pull-in voltage versus depth of the crack locating at  $x_c = 0$ .

Crack depth	$0\mu m$	$0.5\mu m$	$1\mu m$	$1.5\mu m$
$V_{PI}(V)$	38.20	37.7	36.2	34.4

The non-dimensional tip deflection of the cantilever beam versus voltage is shown in Fig. 4. In this case, the crack is located at  $x_c = 0$ . It can be seen as the crack depth increases, the pull-in voltage decreases. Fig. 4 clearly shows that our results for a beam without crack are in good agreement with those of Joglekar and Pawaskar [42].

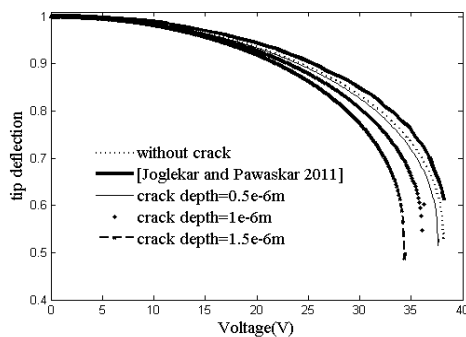


**Fig.4**  
The tip deflection of the cantilever beam as a function of the applied voltage.

Finally, a constant crack depth is considered and the location of the crack is changed. It is observed from Table 5. as the crack approaches the support, the pull-in voltage decreases as a result of stiffness decrease.

**Table 5**  
Pull-in voltage versus position of crack when depth of crack is  $a = 1.5\mu m$ .

Position crack	$x_c = 1$	$x_c = 0.75$	$x_c = 0.25$	$x_c = 0$
$V_{PI}(V)$	38.20	38.2	36.5	34.4

To validate the proposed model, the pull-in voltage is compared with the results cited in the literature for an uncracked beam. Table 6. shows the results of this comparison. As it is seen the result of present work is in good agreement with the others.

**Table 6**  
Comparison of the static pull-in voltage with those cited in the literature in the absence of crack.

Common parameters: $E=169GPa$ , $w=50\mu m$ , $h=3\mu m$ , $g_0=1\mu m$ ( $V_{PI}$ is in $V$ )	
Present work without crack	$V_{PI}=38.2$
Joglekar and Pawaskar [42]	$V_{PI}=38.34$
Osterberg with FE analysis [41]	$V_{PI}=38.2$
Osterberg with 2D model [41]	$V_{PI}=37.9$
Chowdhury et al. [8]	$V_{PI}=37.84$

For further validating the results, the 1DOF model and the beam model results are compared in Fig. 5.

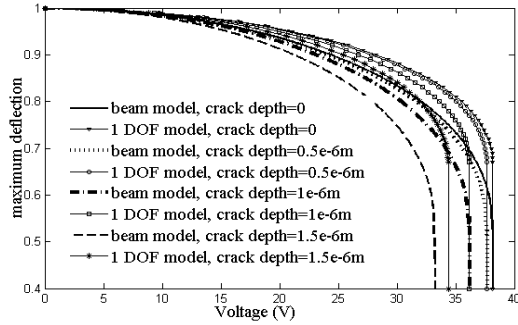


**Fig.5**  
Comparison of the distributed model and 1 DOF model.

It is seen that the results agree relatively well with each other. Noteworthy is that for smaller cracks the pull-in voltage predicted by the lumped model mass model is the same as that obtained from the beam model, however, for longer cracks the results become different. Generally speaking, the beam model results are more reliable for finding the deflection and the pull-in voltage.

5.3 Stability analysis

In this section, the lumped mass model is employed to study the stability of the system. The variations of eigenvalues versus applied voltage are shown in Fig.6. Regarding Fig. 6 (a), it can be seen when the voltage increases from 0 up to a certain value, the eigenvalue  $\lambda(x_{11})$  is pure imaginary for all values of applied voltages indicating neutrally stable fix point. For a larger solution ( $x_{12}$ ) it is clear that the eigenvalues are located on the right-half of the complex plane (Fig. 6 (b)). This indicates that this fix point is an unstable saddle point.

At last, the third eigenvalue  $\lambda(x_{13})$  is pure imaginary (Fig. 6 (c)) and this means that this solution is stable but physically impossible. This is because the non-dimensional amplitude in this case is greater than one ( $x > g_0$ ), which is physically impossible.

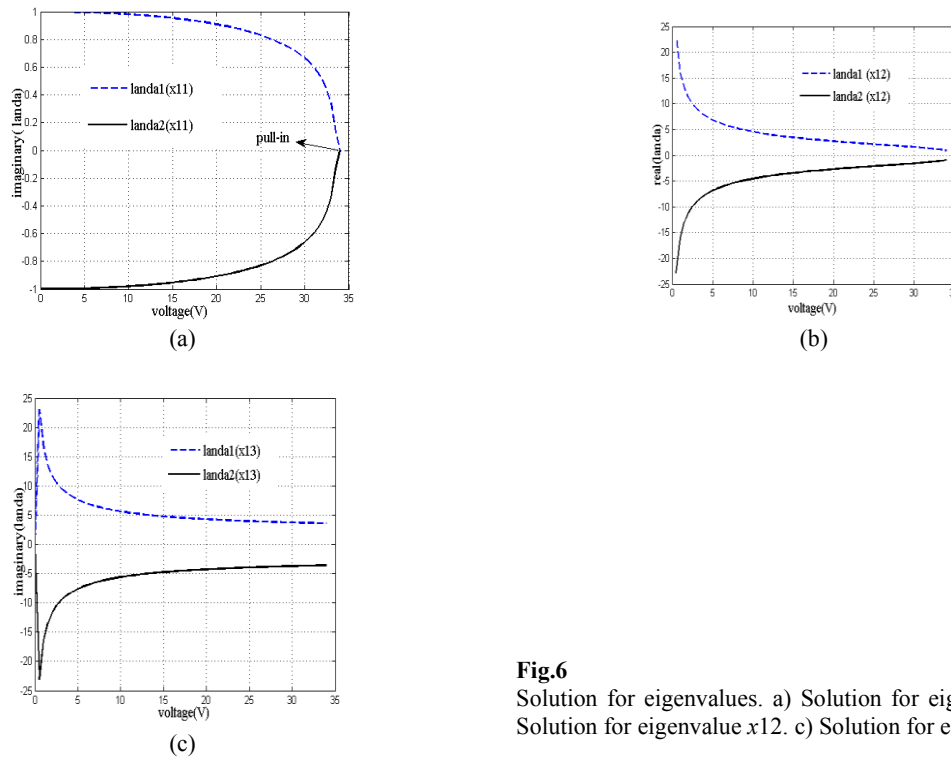


**Fig.6**  
Solution for eigenvalues. a) Solution for eigenvalue  $x_{11}$ . b) Solution for eigenvalue  $x_{12}$ . c) Solution for eigenvalue  $x_{13}$ .

The dynamical behavior of the coupled system corresponding to different initial conditions for a specific crack length ( $L = 100\mu\text{m}$ ,  $x_c = 0.5$ ,  $a = 1.5\mu\text{m}$ ) is shown in the phase portrait of Fig. 7 in three states (it should be noted that the response for  $x$  greater than 1 is not possible physically):

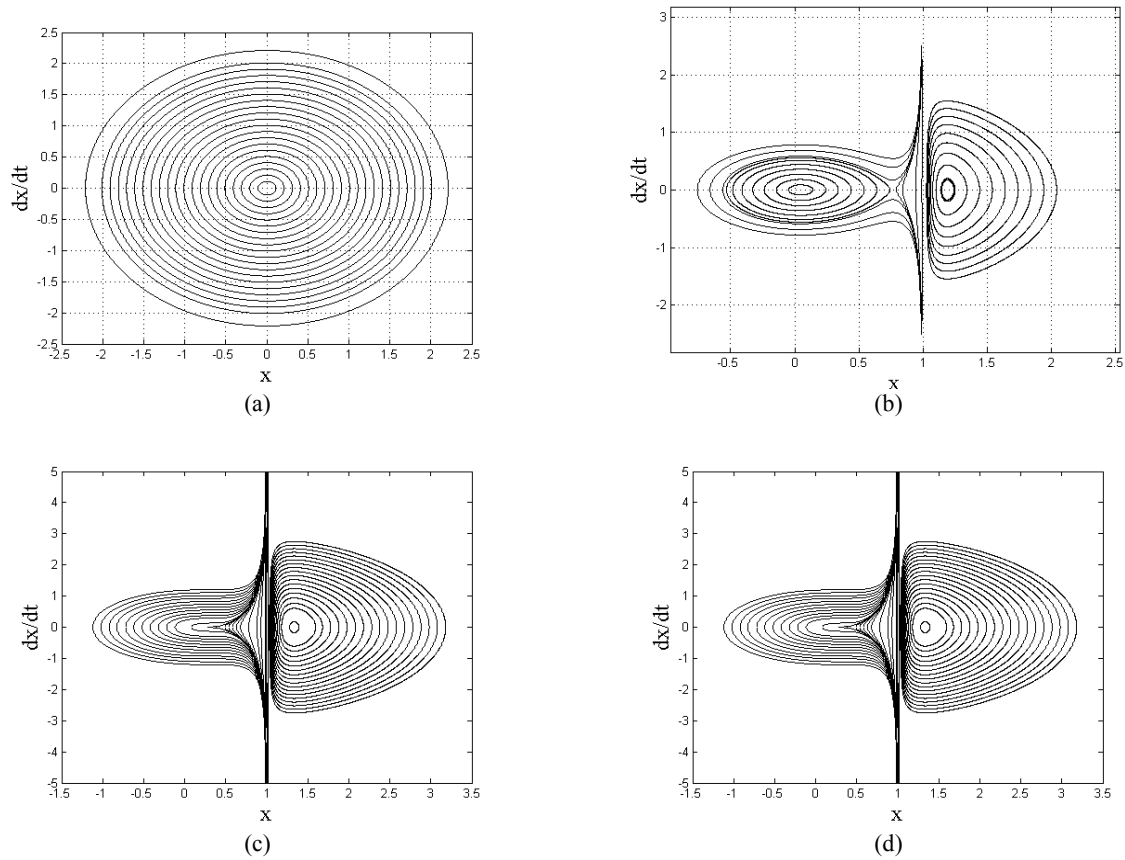


**Fig.7**  
Phase diagram of the 1DOF model. a)  $V=0$ . b)  $V < V_{PI}$ . c)  $V = V_{PI}$ . d)  $V > V_{PI}$ .

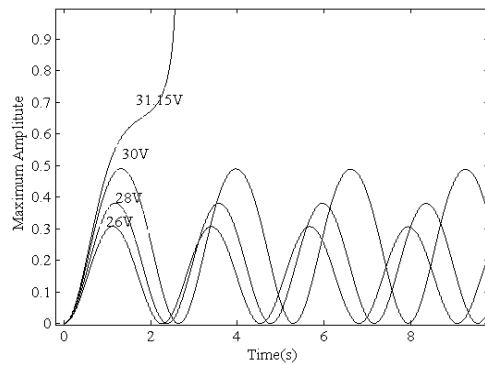
Fig. 7 (a) shows the phase diagram of the pure mechanical model. When no voltage is applied, there exists only one stable center equilibrium position at zero ( $x = 0$ ). The system is stable for any initial conditions.

If the applied voltage is less than the pull-in voltage ( $V < V_{PI}$ ), the system will be stable near the equilibrium position and will oscillate in a non-linear way. If the initial displacement is large enough, the plate will come closer to substrate. It can be seen that even when voltage is below the pull-in voltage, the problem may become unstable. As shown in Fig. 7(b), as the applied voltage approach to a critical value, saddle-node bifurcation is happened. The voltage corresponding to the saddle node bifurcation point is well-known as the static pull-in voltage in MEMS Literature [43] (Fig 7 (b)).

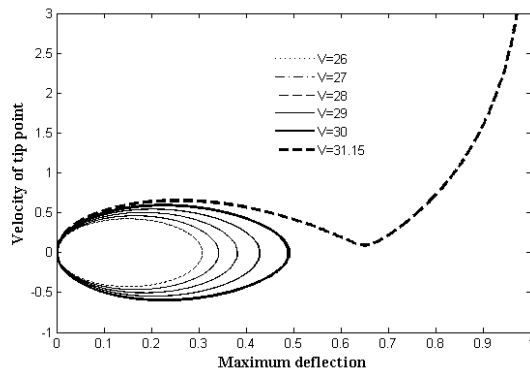
For a voltage higher than the pull-in voltage  $V \geq V_{PI}$  any initial condition leads to instability and the solution becomes divergent (Fig. 7 (c), 7 (d)).

#### 5.4 Dynamic pull-in analysis of the beam model

In the preceding section it is assumed that the DC bias voltage increases slowly to a desired value to avoid the dynamic effect due to the voltage. If the bias voltage is applied within a period smaller than the characteristic time, the dynamic effect due to DC voltage is not negligible and plays an important role. If we solve Eq. (38) for a specific crack length  $L = 100\mu\text{m}$ ,  $x_c = 0.5$ ,  $a = 1.5\mu\text{m}$ . The time history and the phase portrait are obtained as shown in Fig. 8 and 9, respectively.

**Fig.8**

Time variations of the maximum amplitude of the cracked beam due to application of different voltages.

**Fig.9**

Phase diagram of the system for different applied voltages.

Fig. 8 shows that in applied voltages less than 31.15  $V$ , the system has harmonic response versus time, the fact that is verified with the phase diagram (Fig. 9) which shows that in these cases there is a limit cycle for the system. However, as the applied voltage increases to 31.15  $V$ , the system ceases to have a cyclic behavior and instead it experiences very large amplitude which means the instability of the system. So, this voltage is the dynamic pull-in voltage. Lee [37] represents that the pull-in voltage resulted from the dynamic analysis of an un-cracked beam is 91% of the static pull-in voltage of the same beam. Interesting is that the dynamic pull-in voltage of a cracked beam (31.15  $V$ ) is the same percent of the static pull-in voltage (34.4  $V$ ) of the same cracked beam.

## 6 CONCLUSIONS

In this paper the effect of crack on the static and dynamic pull-in phenomena has been investigated. This study shows that with the increase of the crack depth and also approaching the crack to the base point of the beam, the static and dynamic pull-in are happened in low voltages as compared with the case of an un-cracked beam. On the other hand, it was shown that for a cracked beam, especially for longer cracks, the lumped mass model predicts erroneous results and the beam model analysis is necessary instead. The results of this research can also be used for detecting a crack in a beam as a non-destructive testing procedure.

## REFERENCES

- [1] Senturia S. D., 2001, *Microsystem Design*, Boston, Kluwer.
- [2] Younis M. I., Nayfeh A. H., 2003, A study of the nonlinear response of a resonant micro-beam to an electric actuation, *Journal of Nonlinear Dynamics* **31**: 91-117.
- [3] Elata D., Bamberger H., 2006, On the dynamic pull-In of electrostatic actuators with multiple degrees of freedom and multiple voltage sources, *Journal of Microelectromechanical Systems* **15**: 131-140.
- [4] Zhang Y., Zhao Y., 2006, Numerical and analytical study on the pull-in instability of micro-structure under electrostatic loading, *Sensors and Actuators A: Physical* **127**: 366-380.
- [5] Rezazadeh G., Fathaliou M., Sadeghi M., 2011, Pull-in voltage of electro-statically actuated micro-beams in terms of lumped model pull-in voltage using novel design corrective coefficients, *Sensing and Imaging* **12**: 117-131.

- [6] Zhang W. M., Yan H., Peng Z. K., Meng G., 2014, Electrostatic pull-in instability in MEMS/NEMS: a review, *Sensors and Actuators A: Physical* **214**: 187-214.
- [7] Choi B., Lovell E. G., 1997, Improved analysis of micro-beams under mechanical and electrostatic loads, *Journal of Micromechanics and Micro engineering* **7**: 24-29.
- [8] Chowdhury S., Ahmadi M., Miller W. C., 2005, A closed-form model for the pull-in voltage of electrostatically actuated cantilever beams, *Journal of Micromechanics and Micro engineering* **15**: 756-763.
- [9] Chao P. C. P., Chiu C. W., Liu T. H., 2008, DC dynamic pull-in predictions for a generalized clamped-clamped micro-beam based on a continuous model and bifurcation analysis, *Journal of Micromechanics and Micro engineering* **18**: 1-14.
- [10] Krylov S., 2007, Lyapunov exponents as a criterion for the dynamic pull-in instability of electrostatically actuated microstructures, *International Journal of Non-Linear Mechanics* **42**: 626-642.
- [11] Varvani-Farahani A., 2005, Silicon MEMS components: a fatigue life assessment approach, *Microsystem Technologies* **11**: 129-134.
- [12] Hill M J., Rowcliffe D. J., 1947, Deformation of silicon at low temperatures, *Journal of Materials Science* **9**: 1569-1576.
- [13] Muhlstein C. L., Brown S. B., Ritchie R. O., 2001, High-cycle fatigue and durability of polycrystalline silicon films in ambient air, *Sensors and Actuators A: Physical* **94**: 177-188.
- [14] Ando T., Shikida M., Sato K., 2001, Tensile-mode fatigue testing of silicon films as structural materials for MEMS, *Sensors and Actuators A: Physical* **93**: 70-75.
- [15] Motallebi A., Fathalilou M., Rezazadeh G., 2012, Effect of the open crack on the pull-in instability of an electrostatically actuated micro-beam, *Acta Mechanica Solida Sinica* **25**: 627-637.
- [16] Sourki R., Hoseini S. A. H., 2016, Free vibration analysis of size-dependent cracked micro-beam based on the modified couple stress theory, *Applied Physics A* **413**: 1-11.
- [17] Tadi Beni Y., Jafaria A., Razavi H., 2015, Size effect on free transverse vibration of cracked nano-beams using couple stress theory, *International Journal of Engineering* **28**: 296-304.
- [18] Loya J. A., Aranda-Ruiz J., Fern J., 2014, Torsion of cracked Nano-rods using a nonlocal elasticity model, *Journal of Physics D: Applied Physics* **47**: 115304-115315.
- [19] Barr A. D. S., Christides S., 1984, One-dimensional theory of crack Euler-Bernoulli beams, *International Journal of Mechanical Sciences* **26**: 639-639.
- [20] Rizos P. F., Aspragathos N., Dimarogonas A. D., 1990, Identification of crack location and magnitude in cantilever beam from the vibration modes, *Journal of Sound Vibration* **138**: 381-388.
- [21] Chondros T. G., Dimarogonas A. D., Yao J., 1998, A continuous cracked beam vibration theory, *Journal of Sound Vibration* **215**: 17-34.
- [22] Behzad M., Meghdari A., Ebrahimi A 2008 A linear theory for bending stress-strain analysis of a beam with an edge crack, *Engineering Fracture Mechanics* **75**: 4695-4705.
- [23] Li Q. S., 2002, Free vibration analysis of non-uniform beams with an arbitrary number of cracks and concentrated mass, *Journal of Sound Vibration* **252**: 509-525.
- [24] Binici B., 2005, Vibration of beams with multiple open cracks subjected to axial force, *Journal of Sound Vibration* **287**: 277-295.
- [25] Zhang G. P., Wang Z. G., 2008, Fatigue of small-scale metal materials: from micro to nano-scale structural integrity and microstructural worthiness, *Springer Netherlands* **152**: 275-326.
- [26] Sadeghian H., Goosen H., Bossche A., Thijse B., Van Keulen F., 2011, On the size-dependent elasticity of silicon nano-cantilevers: impact of defects, *Journal of Physics D: Applied Physics* **44**: 072001.
- [27] Shengli K., Shenjie Z., Zhifeng N., Kai W., 2009, Static and dynamic analysis of micro beams based on strain gradient elasticity theory, *International Journal of Engineering Science* **47**: 487-498.
- [28] Zamanzadeh M., Rezazadeh G., Jafarsadeghi-poornaki I., Shabani R., 2013, Static and dynamic stability modeling of a capacitive FGM micro-beam in presence of temperature changes, *Applied Mathematical Modeling* **37**: 6964-6978.
- [29] Akbaş S. D., 2016, Free vibration of edge cracked functionally graded micro-scale beams based on the modified couple stress theory, *International Journal of Structural Stability and Dynamics* **16**: 1750033.
- [30] Torabi K., Dastgerdi J., 2012, An analytical method for free vibration analysis of Timoshenko beam theory applied to cracked nano-beams using a nonlocal elasticity model, *Thin Solid Films* **520**: 6595-6602.
- [31] Gounaris G. D., Papadopoulos C. A., Dimarogonas A. D., 1996, Crack identification in beams by coupled response measurement, *Computational and Structural* **58**: 409-423.
- [32] Shifrin E. I., Ruotolo R., 1999, Natural frequencies of a beam with an arbitrary number of cracks, *Journal of Sound Vibration* **223**: 409-423.
- [33] Dimarogonas A. D., Paipettis S. A., 1983, *Analytical Methods in Rotor Dynamics*, Elsevier Applied Science, London.
- [34] Dimarogonas A. D., 1976, *Vibration Engineering*, Paul, West Publishers.
- [35] Rezazadeh G., Tahmasebi A., Zubostow M., 2006, Application of piezoelectric layers in electrostatic MEM actuators: controlling of pull-in voltage, *Microsystem Technologies* **12**: 1163-1170.
- [36] Dominicus J., Ijntema Harrie A. C., 1992, Static and dynamic aspects of an air-gap capacitor, *Sensors and Actuators A: Physical* **35**: 121-128.
- [37] Lee K. B., 2011, *Principles of Micro-Electromechanical Systems*, John Wiley & Sons, New Jersey.

- [38] Younis M. I., 2011, *MEMS Linear and Nonlinear Statics and Dynamics*, Springer, New York.
- [39] Rochus V., Rixen D. J. and Golinval J.C., 2005, Electro-static coupling of MEMS structures: transient simulations and dynamic pull-in, *Nonlinear Analysis, Theory, Methods & Applications* **63**: 1619-1633.
- [40] Vytautas O., Rolanas D., 2010, *Microsystems Dynamics*, Springer, New York.
- [41] Osterbeg P. M., 1995, *Electro-Statically Actuated Micro-Electromechanical Test Structures for Material Property Measurements*, PhD Dissertation Massachusetts Institute of Technology.
- [42] Joglekar M. M., Pawaskar D. N., 2011, Closed-form empirical relations to predict the static pull-in parameters of electrostatically actuated micro-cantilevers having linear with variation, *Microsystem Technologies* **17**: 35-45.
- [43] Abbasnejhad B., Rezazadeh G., Shabani R., 2011, Stability analysis of a capacitive FGM micro-beam using modified couple stress theory, *Acta Mechanica Solida Sinica* **26**: 427-440.